Assessment of the current density evolution during an ELM cycle using beam emission polarimetry at ASDEX Upgrade

R. Dux[1], E. Viezzer[2], M. Cavedon[1], M. G. Dunne[1], R. Fischer[1],
and the ASDEX Upgrade team

[1]*Max-Planck-Institut für Plasmaphysik, Garching, Germany*
[2]*Dept. of Atomic, Molecular and Nuclear Physics, University of Seville, Spain*

The knowledge of the current density in the pedestal region of H-mode plasmas is important to understand the stability of the pedestal with respect to edge localised modes (ELMs). The current density is connected to the poloidal magnetic field B_p via Ampères law, which can be determined by an accurate measurement of the field line angle $\gamma = \arctan(B_p/B_t)$ where B_t is the toroidal magnetic field. In an H-mode discharge with low frequency type-I ELMs, the evolution of the γ-profiles in the pedestal region has been measured with the beam emission polarimetry (BEP) diagnostic at ASDEX Ugrade.

Diagnostic Setup

The D_α line of fast neutral beam atoms is split due to an electric field in the rest frame of the atoms (motional Stark effect). This electric field $\vec{F}$ is given by the velocity of the fast atoms $\vec{v}$ and the magnetic field $\vec{B}$: $\vec{F} = \vec{v} \times \vec{B}$ and might also have a small contribution from the radial electric field in the H-mode edge. The multiplet contains in the centre σ-lines, which are polarised perpendicular to the electric field, and π-lines, which are polarised parallel to the electric field. The BEP diagnostic [1] determines their polarisation direction at 5 spatial locations at the plasma edge covering ≈8 cm. Three independent observations of each spatial location are used, where each optical head includes a polariser, which is roughly oriented at 0^o, 45^o, and 90^o with respect to the electric field. The full multiplet is measured with a spectrometer with 3 ms time resolution. The $0^o/90^o$ channel serves as a reference for the strength of the π-/σ-lines, while the 45^o channel yields via radiance variations of the π- and σ-lines information about changes of the electric field direction, which are connected to changes in the direction of the magnetic field. The line radiance of the transition i of D_α emitted by beam neutrals (of one specific energy) with a polarisation angle α between $\vec{F}$ and the electric field of the light wave is given by an integral over the line-of-sight (LOS), which for σ- and π-lines just differs by an angle factor, which is here denoted with the value of the pure Stark effect.

$$L_{\sigma,i} = \frac{1}{4\pi}\int_{LOS} n(l) r(l) f_i \sin^2\alpha \, dl \quad L_{\pi,i} = \frac{1}{4\pi}\int_{LOS} n(l) r(l) f_i \cos^2\alpha \, dl \tag{1}$$

Here, $n(l)$ is the number density of the unattenuated beam neutrals, $r(l)$ is the total rate of emitted D_α photons per injected beam atom, f_i is the relative strength of transition i, which usually differs from the known values obtained with thermally equilibrated occupation of the upper levels [2]. The deviation of f_i from the thermal equilibrium is described by 3 non-thermal occupation numbers, which deliver f_i for all 9 lines. The line radiance yields with the sensitivity s_{LOS} a count rate $\dot{c}_i = s_{LOS} L_i$ at the CCD camera of the spectrometer. Since the variation of the

signal with the polariser orientation is measured on individual LOS, all factors that can influence $\dot{c}_i$ besides the change of α need to be taken into account.

The sensitivity of each LOS is determined by measuring the count rates when illuminating the optical heads with a calibrated light source. The relative signals of the individual LOS are then measured by injecting the beam into the gas filled torus without any magnetic field. Here, the excitation of the beam atoms is in an equilibrium and the photon rate r is a constant. There is no splitting into Stark components and the count rates are: $\dot{c} = s_{LOS} r/(4\pi) \int n(l) dl$, where $\int n(l) dl$ is calculated from a beam model which takes the beam source geometry, the vertical and horizontal focal length and the angular spread of the beam into account. The model delivers a small variation of $\int n(l) dl$ around the value for the central LOS, which reaches up to $\pm 4\%$ for the outer LOS. The measured D_α distribution shows some scatter around the results of the beam model with a maximum deviation of 5%. It is used to refine the sensitivity values for each LOS.

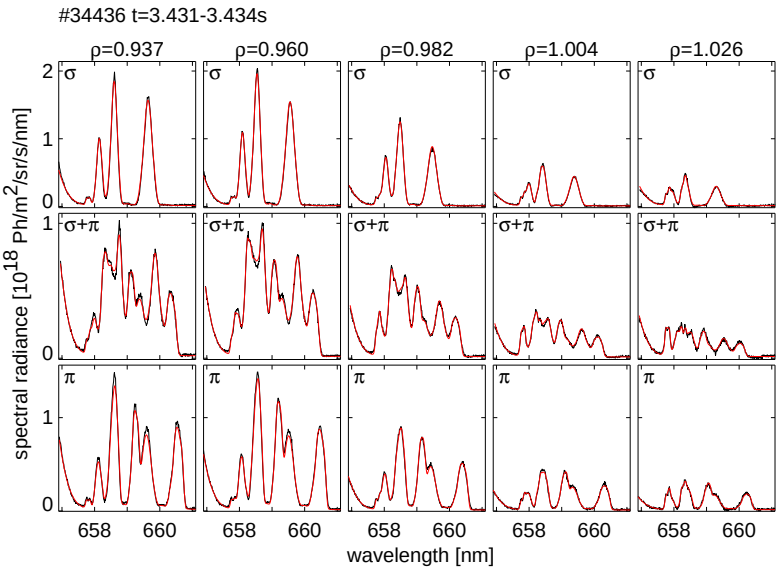

Fig.1: *The measured spectra (black) and the fit (red) for all radial positions (columns) and the three polariser orientations (rows). The upper row with $\alpha \approx 90^o$ shows mainly σ-lines, the middle row with $\alpha \approx 45^o$ π- and σ-lines and the lower row with $\alpha \approx 0^o$ just π-lines.*

In H-mode plasma discharges, the photon rate r strongly increases within the edge transport barrier (roughly with the main ion density) and becomes much flatter after an ELM. A numerical model of the beam emission in that region showed, that r is sufficiently well described when using a dependence on the flux surface coordinate only. Furthermore, the model revealed that a strong r gradient introduces radiance variations of the 0^o- and 90^o-channel with respect to the corresponding 45^o-channel of up to $\pm 5\%$. Thus, the actual r-profile has to be determined within the fit procedure.

Fit procedure

The fit procedure of the obtained spectra is performed in three steps. In the first step, the spectra of three LOS which observe the same radial location through different polarisers are fitted together. For the Stark multiplets of the full, half and third energy component of the beam, the total D_α line radiance is an individual fit parameter. The non-thermal occupation of the upper level is taken to be equal for the three LOS and also the field line angle, which determine the relative intensities of the individual lines. Furthermore, the spectral radiance of the continuum emission, the red wing of the passive D_α-emission around 657 nm and the radiance of the CII dou-

blet at 657.8 nm and 658.3 nm are individual fit parameters for each LOS. In the next step, signal combinations, which are insensitive to the exact values of α and f_i are formed, i.e. $L_{45} = \sum L_{i,45}$ and $L_{0+90} = \sum (L_{i,0} + L_{i,90})$, and are fitted using a common profile $r(\Psi)$. In the third step, the spectra of three LOS are fitted again but now the total D_α line radiance comes from the line integral using $r(\Psi)$. The non thermal occupation numbers, the radiance of CII, the passive D_α and the continuum background are taken from the old fit. Here, the field line angle is effectively the only free remaining fit parameter. In all fits, the small influence of E_r is taken into account using CXRS-measurements. The quality of the fit is very good as is shown in Fig. 1 for a single exposure during the inter-ELM phase of discharge #34336.

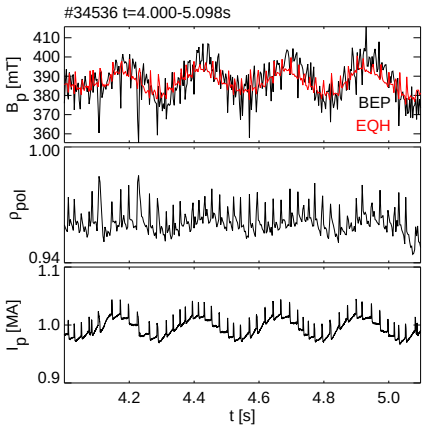

Fig.2: *The temporal change of B_p from BEP and the equilibrium reconstruction agree well on the innermost BEP channel for a discharge with a ±2% modulation of I_p.*

Experimental Results

In an H-mode discharge with a pre-programmed modulation of I_p of ±20 kA around the mean value of 1 MA (lowest graph in Fig.2), the evolution of B_p on the innermost channel of the BEP diagnostic at a normalised poloidal flux label ρ_{pol}≈0.96 (middle graph of Fig. 2) reproduces well the modulation from the equilibrium reconstruction (upper graph in Fig.2).

In the type-I ELMy H-mode discharge #34436 with constant I_p=1 MA, B_t=-2.5 T, P_{NBI}=5 MW and P_{ECRH}=1.2 MW the evolution of the B_p profile in the pedestal region during an ELM cycle could be measured. The discharge had a radial sweep of the plasma column by 1 cm to obtain a dense radial grid of BEP measurements. The data measured from 3 to 6.5 s were considered, where there were 124 ELMs, but only the 67 most similar ELM periods were selected for further analysis. The selection was based on a correlation analysis of the divertor shunt current I_{SOL} evolution. The selected ELMs cause an energy loss of ΔW_{ELM}=50 kJ and the mean period is 28 ms. I_{SOL} is shown in the lowest graph of Fig. 3. The BEP data were grouped in 1 ms wide time bins using the time difference of the measurement time t to the ELM onset time $\Delta t_{ELM} = t - t_{onset}$, where t is the centre of the 3 ms long integration time of the CCD camera. The profiles of r and B_p within each bin were fitted to obtain the mean profile and the temporal evolution of the mean values at ρ_{pol}=0.96 (pedestal top) and 1. These mean values are shown in Fig. 3. With the ELM, the profile of the photon rate, which is roughly proportional to the main ion density profile, and

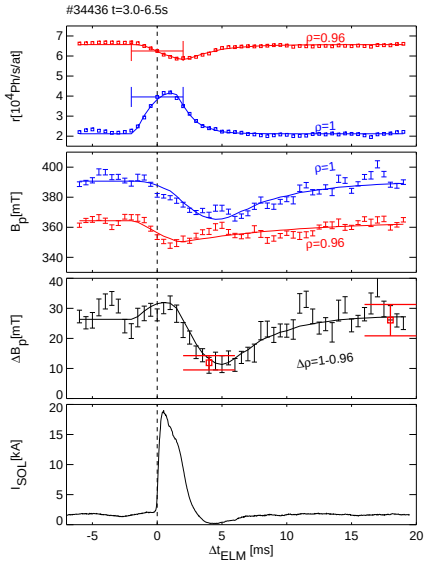

Fig.3: *The evolution of r and B_p from BEP at ρ_{pol}=0.96 and 1 and of $\Delta B_p = B_p(1) - B_p(0.96)$ are shown for 3 ms wide time bins. The red stars depict the results from pressure constrained equilibrium reconstructions.*

of B_p flatten and subsequently recover to the pre-ELM value. The evolution of B_p during both phases is much slower than of r.

A fit to the data of r and B_p with 4 ms-averages of a simple function, which changes linearly in time from the pre-ELM value at Δt_{ELM}=0 to a peak value and then exponentially decays back, yields the solid lines in the graphs. The poloidal field difference ΔB_p between ρ_{pol}=1 and 0.96 is shown in the third graph of Fig.3. The solid line is just the difference of the two fit functions for B_p. ΔB_p is about 25 mT at the end of the recovery. This is much more than calculated from standard equilibrium reconstruction. Fitting pedestal profiles of n_e, T_e and T_i profiles after an ELM and after the recovery allowed to calculate equilibria which are constrained by the edge pressure profiles and the SOL currents [3]. The ΔB_p values for these equilibria (EQB) are in good agreement with the measured values and are shown as red squares in Fig. 3. We ascribe a 20% uncertainty to the equilibrium values due to the uncertainties of the pressure profile, since the toroidal current is mainly driven by the pressure gradient as is shown below. For the pre-ELM equilibrium reconstruction, the B_p profile at the location of the BEP measurements (outboard side, 30 cm below the magnetic axis) is shown in the lower panel of Fig. 4. The absolute B_p values from EQB are 48 mT below the BEP result and the B_p traces in Fig.3 have already been corrected using this offset. The reason for the shift is under investigation. Fig. 4 shows also the profiles of pressure and toroidal current densities from EQB at this location (solid lines). The strongest contribution to j_{tor} delivers the Pfirsch-Schlüter (PS) current, then comes the sum of bootstrap (BS), ohmic and externally driven current, and finally the low diamagnetic current. In addition, BS-, PS- and diamagnetic current from a neo-classical calculation with a similar pressure profile is depicted in Fig.4 using lines with crosses. By comparison of the profiles, it can be concluded that the ohmic and current drive contribution is about 50% of the BS-part. The local bootstrap current at this outboard side location amounts only to about 22% of the total toroidal current density and the BEP measurements are not very sensitive to test models of the bootstrap current in this region.

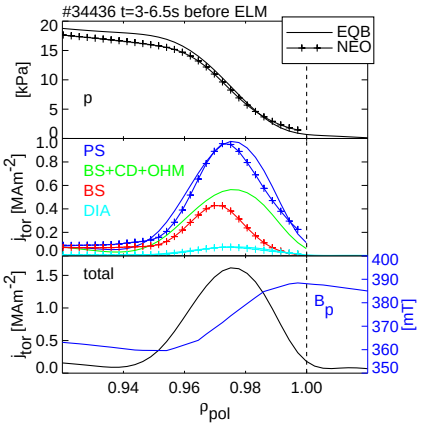

Fig.4: *Profiles of pressure, toroidal current densities and B_p at the location of the BEP diagnostic from EQB and a neoclassical code calculation.*

Acknowledgement

This work has been carried out within the framework of the EUROfusion Consortium and has received funding from the Euratom research and training programme 2014-2018 and 2019-2020 under grant agreement No 633053. The views and opinions expressed herein do not necessarily reflect those of the European Commission.

References

[1] E. Viezzer, R. Dux et al, Rev. Sci. Instrum.**87** (2016) 11E528.
[2] O. Marchuk et al, J. Phys. B: At. Mol. Opt. Phys. **43** (2010) 011002.
[3] M. G. Dunne et a Nucl. Fusion **52** (2012) 123014.